Reduction of the BTI Time-Dependent Variability in Nanoscaled MOSFETs by Body Bias

J. Franco, B. Kaczer, M. Toledano-Luque, Ph. J. Roussel, G. Groeseneken[1]
imec
Leuven, Belgium
Phone: +32 16 28 10 85, e-mail: Jacopo.Franco@imec.be
[1]also with ESAT, KU Leuven, Belgium

B. Schwarz, M. Bina, M. Waltl, P.-J. Wagner, T. Grasser
Institute for Microelectronics, T.U. Wien
Wien, Austria

***Abstract*—We study the impact of individual charged gate oxide defects on the characteristics of nanoscaled pMOSFETs for varying body biases. Both a reduced time-zero variability and a reduced time-dependent variability are observed when a forward body bias is applied. In order to explain these observations, a model based on the modulation of the number of unscreened dopant atoms within the channel depletion region is proposed.**

Keywords-Body Bias, Nanoscale, Negative Bias Temperature Instability, pMOSFETs, Variability.

I. INTRODUCTION

With the aggressive scaling of CMOS device size, the number of dopant atoms *and* the number of defects in each device reduces to numerable levels [1]. This trend has significant technological implications: it results in increased *time-zero* (i.e., as-fabricated) variability, but also considerable *time-dependent* variability (i.e., reduced reliability) [2,3]. Several groups have recently shown that the properties of individual charged gate oxide defects (e.g. capture and emission times) can be directly observed and measured in deeply scaled MOSFETs [4-7]. We have recently studied the impact of individual defects on the I_D-V_G characteristics of nanoscaled pMOSFETs and found that each defect causes a V_G-dependent threshold voltage shift (ΔV_{th}) [8]. In particular we observed that the detrimental impact of defects causing a relevant shift of the device characteristic close to V_{th} is reduced at higher V_G's of relevance for device operation [8,9].

In this work we show that the body bias also modulates the impact of individual charged defects on the device characteristics. A reduced time-zero V_{th}-variability and reduced single-defect-induced ΔV_{th}'s are observed when applying a forward body bias. We ascribe these observations to a reduced sensitivity to current percolation paths and we propose a model based on the modulation of unscreened dopant atoms within the channel depletion region which quantitatively explains the reduced impact of individual charged defects.

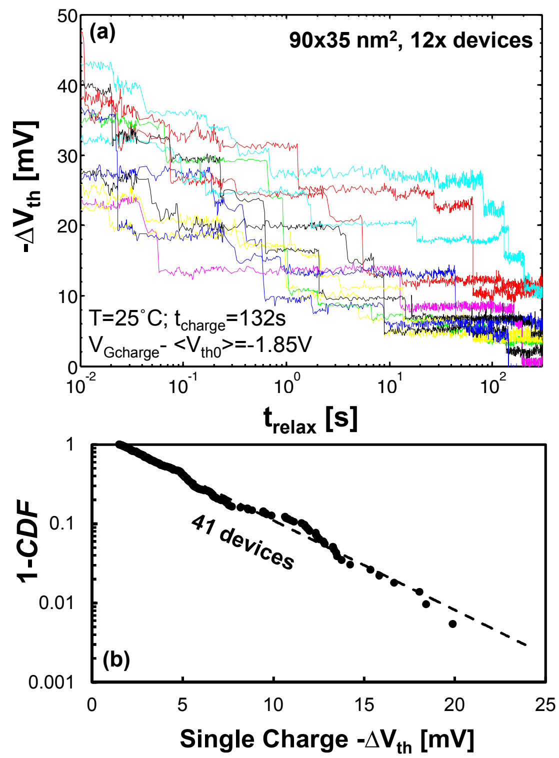

Figure 1. (a) NBTI-like relaxation transients recorded on nanoscaled (~90x35nm^2) Si pMOSFETs. The total ΔV_{th} strongly varies from device to device [3]. Individual gate oxide defect discharge events are visible, with varying ΔV_{th} step heights. (b) The ΔV_{th} step heights appear exponentially distributed, with the average step height η depending on the device dimensions [8], oxide thickness and doping level [10], see Eq. (2).

II. EXPERIMENTAL

We performed Negative Bias Temperature Instability (NBTI) like experiments at room temperature on nanoscaled (~90x35nm^2) Si/SiON/poly-Si (CET$\approx$2nm) pFETs: after a defect charging phase, relaxation transients were recorded [Fig. 1 (a)].

978-1-4799-0113-5/13/$31.00 ©2013 IEEE

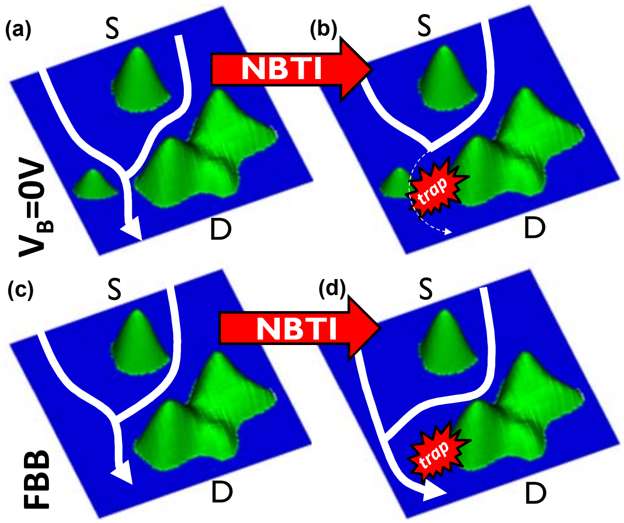

Figure 2. (a) RDD causes a non-uniform potential profile in the channel. The carrier conduction hence proceeds through percolation paths (sketches generated via [11]). (b) In the unlucky case of a charged gate oxide defect located above the constriction point, the percolation path will be blocked off, causing a strong reduction in the current (i.e., a large ΔV_{th} step, see Fig. 1). (c) For a reduced X_{dep} obtained by applying a FBB, fewer unscreened dopant atoms might be included in the depletion layer (d) reducing the sensitivity to the current percolation effect.

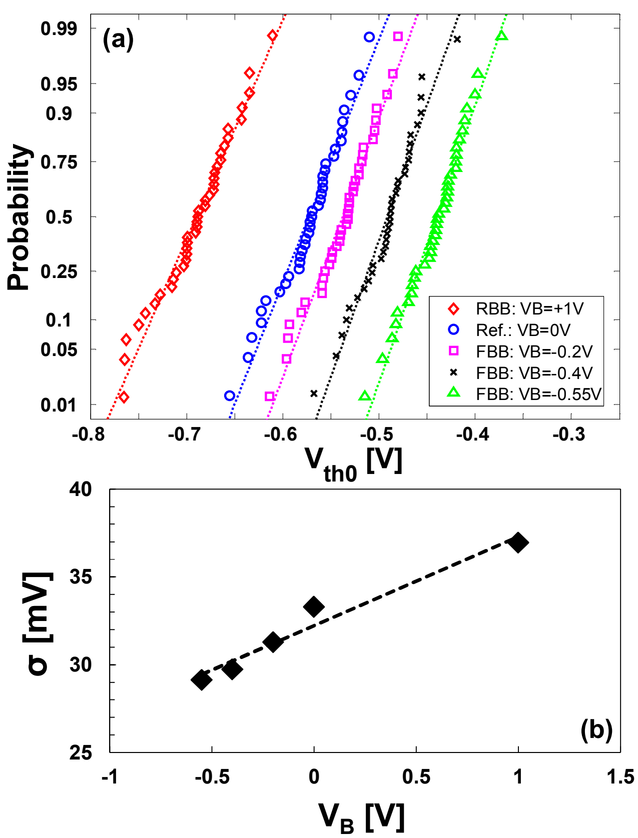

Figure 3. (a) Probability plot of the initial V_{th0}'s of a set of nanoscaled devices for different V_B's, following normal distributions. The BB modulates both the average V_{th0} and (b) its variability, with a FBB reducing the standard deviation of the normal distribution.

The total ΔV_{th} observed after the same NBTI stress strongly varies from device to device [3]. Individual gate oxide defect discharge events are visible in the relaxation traces, and the associated ΔV_{th} step heights appear approximately exponentially distributed [Fig. 1 (b)] with *CDF*:

$$F(\Delta V_{th},\eta)=1-\exp\left(-\frac{\Delta V_{th}}{\eta}\right), \quad (1)$$

where η is the average ΔV_{th} step height. Note individual charged defects causing remarkable ΔV_{th} up to ~20mV when charged. Such anomalous single-defect-induced ΔV_{th}'s are ascribed to the percolative nature of the current flow in the channel yielded by the non-uniform potential profile resulting from Random Dopant Distribution (RDD) [1] in nanoscaled FETs [see Fig. 2 (a)]. A charged gate oxide defect located on top of a critical spot (i.e., the point of maximum confinement) might block off the percolation path and cause a significant current reduction [Fig. 2 (b)], observed as a large threshold voltage shift. The average ΔV_{th} step height η, i.e., *the average impact of a single charged defect on the FET behavior*, is expected to scale inversely with the device channel area [8], and proportionally with the gate oxide thickness t_{ox} and the square root of the dopant concentration in the channel N_D [10]:

$$\eta \propto \frac{t_{ox}\sqrt{N_D}}{WL}. \quad (2)$$

The body bias (BB) technique is commonly used to modulate the channel depletion layer thickness (X_{dep}) and therefore the V_{th0} of the MOSFET devices. A reverse body bias (RBB) increases X_{dep} and $|V_{th0}|$ and can be exploited for low leakage applications, while a forward body bias (FBB) reduces X_{dep} and $|V_{th0}|$, which can be favorable for high performance applications, at the cost of increased junction leakage [12]. We found that the BB has also a significant impact on both the time-zero and the time-dependent variability of scaled devices, as discussed next.

III. Results

Measurements of the initial V_{th0}'s of a device sample set revealed normal distributions and showed that the applied BB not only modulates the average threshold voltage value but also the V_{th0}-variability, with a FBB reducing the standard deviation of the V_{th0} distribution (Fig. 3). This observation suggests that reducing the X_{dep} by means of BB might yield the same beneficial effect on the time-zero variability as reducing the channel doping level N_D. It is of interest hence to investigate the effect of BB on the time-dependent variability, specifically evaluating the impact of individual charged oxide defects on the device V_{th} for different V_B's. Fig. 4 (a) gives NBTI relaxation traces recorded for different BB on one device manifesting a single dominant oxide trap ($\Delta V_{th}\approx$25mV) [8]: *the BB modulates the* ΔV_{th} *step height associated with the trap charging/discharging*, with a lower step height for the FBB cases and a higher step height for the RBB case. The same observation was consistently repeated on several devices manifesting such dominant gate oxide defects [Fig. 4 (b)].

Furthermore, the same trend was clearly confirmed by looking at the *entire distributions* of the single charge step heights observed on multiple devices (Fig. 5), with a reduced average ΔV_{th} step height η for the FBB cases. The extraction of η for different BB was repeated on two different wafers (both having a Si/SiON/poly-Si gate stack but with slightly different oxide thickness) and for two different charging conditions [Fig. 6 (a)]. When normalizing the extracted η values to the respective $V_B = 0$V cases, a universal trend is found [Fig. 4 (b)], with a measured reduction in η down by -25% for a FBB as low as $V_B = -0.6$V.

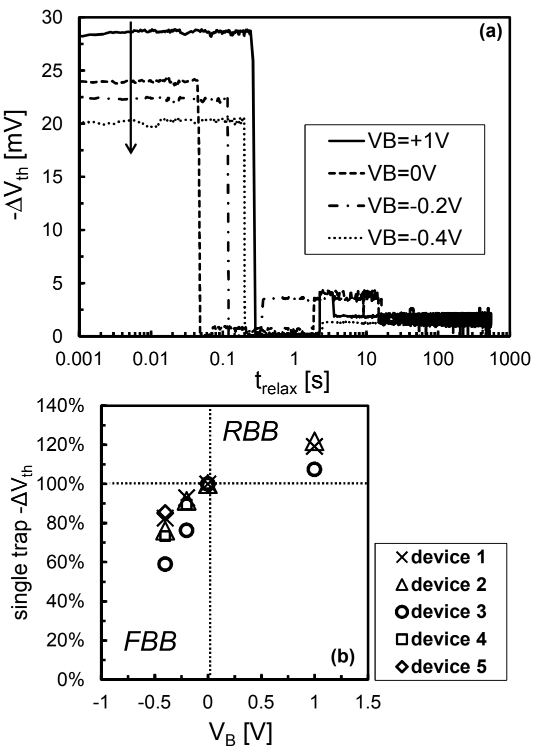

Figure 4. (a) NBTI relaxation traces recorded for different BB on one selected device showing a single dominant oxide trap (ΔV_{th}≈25mV): the BB modulates the ΔV_{th} step height, with a FBB reducing it. (b) The same observation is consistently repeated on several such devices showing single dominant oxide traps.Previous works suggested that also the defect capture and emission times can be dependent on the BB [13]

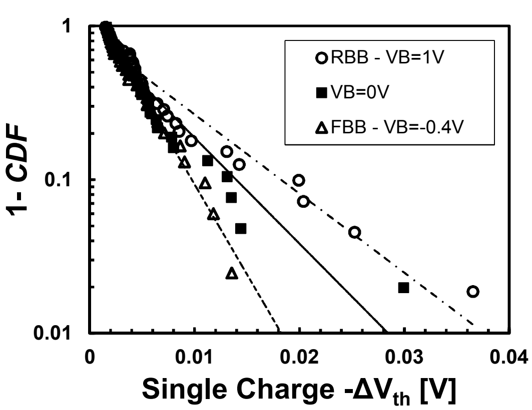

Figure 5. Exponential distributions of the single charge ΔV_{th} step heights obtained on the same sample set for different applied V_B's. Note the increased variance (larger η) for the RBB case and the reduced variance (smaller η) for the FBB case.

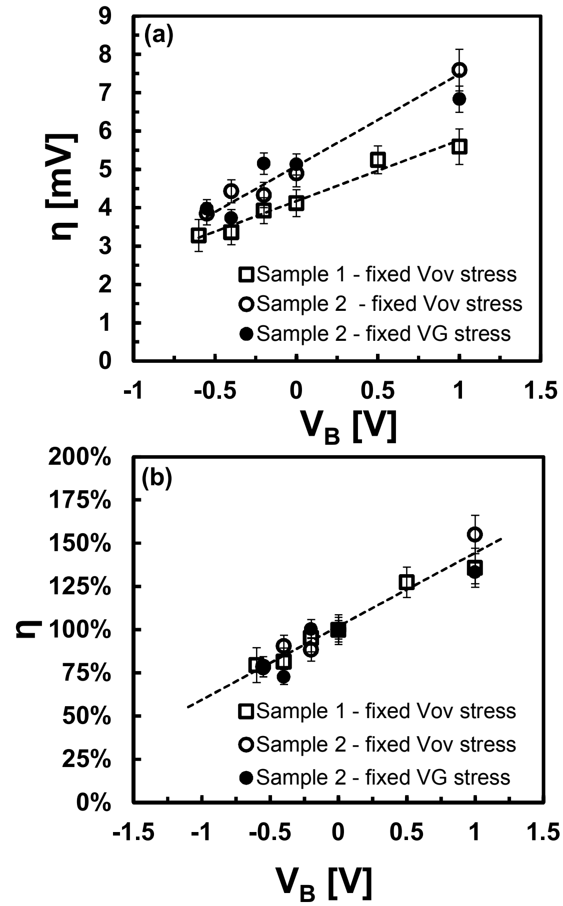

Figure 6. (a) η values extracted with a Maximum Likelihood fit from the distributions measured for varying BB (see Fig. 5) on two wafers with identical Si/SiON/Poly-Si gate stack and identical doping levels, but slightly different oxide thicknesses (CET 1.8~2.1nm). On Sample 2, the NBTI-like defect charging phase was performed at two different gate biases: at fixed gate overdrive stress voltage (i.e. constant inversion hole population but lower oxide electric field E_{ox} for the FBB, [14]), and at fixed gate stress voltage (i.e. same E_{ox} but varying hole population for different BB, [14]). In every case the FBB was found to reduce η while the RBB increased it. (b) When normalizing the η values to the respective V_B = 0V standard cases, a universal trend is found.

IV. Discussion

We interpret these experimental observations as related to the BB modulation of X_{dep}. For a reduced X_{dep} (FBB), a reduced number of unscreened dopant atoms is included in the depletion layer [Fig. 2 (c), cf. (a)], reducing the sensitivity to current percolation paths [Fig. 2 (d), cf. (b)], while for a wider X_{dep} more dopant atoms can contribute to the non-uniformity of the potential profile in the channel. In other words, *reducing the X_{dep} by means of BB alleviates the RDD effects and improves the time-zero and the time-dependent variability as effectively as reducing the channel doping level.* To support this hypothesis, we calculated the average number of dopant atoms (n_D) located within the channel depletion width as a function of the BB as:

$$n_D = WLN_DX_{dep} \ , \qquad (3)$$

where W and L are the device width and length respectively, and N_D is the channel doping level.

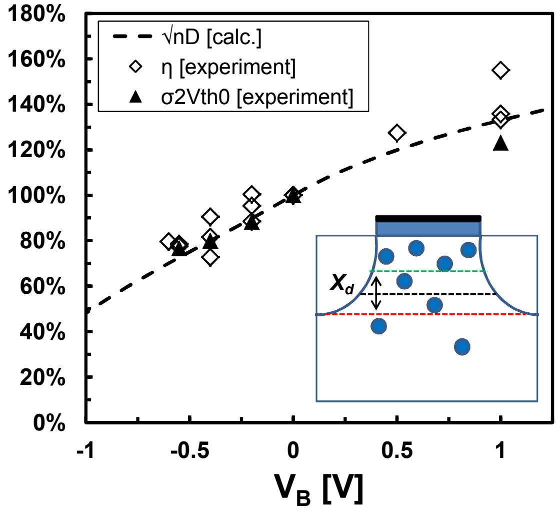

Figure 7. (Inset) The body bias modulates the channel depletion width [X_{dep}, see Eq. (4)] and therefore the average number of unscreened dopant atoms within the depletion layer [n_D, see Eq. (3)]. The average ΔV_{th} step height (η) and the variance of the V_{th0} distribution (σ^2_{Vth0}) are expected to scale proportionally with the square root of the channel doping concentration (see Eq. (2), [10,16]). The measured modulations of η and of σ^2_{Vth0} by BB (symbols) are excellently correlated to the calculated square root of n_D (dashed line) over the whole considered V_B range. This observation suggests BB as a flexible electrical equivalent to doping level adjustment.

The channel depletion layer thickness X_{dep} was calculated as a function of V_B according to textbook equations [15] as:

$$X_{dep} = \sqrt{\frac{2\varepsilon_0 \varepsilon_{Si}}{qN_D}(\phi_s + V_B)}\ , \tag{4}$$

$$\phi_s = V_T \ln\left(\frac{N_D}{n_i}\right)\ , \tag{5}$$

where V_T is the thermal voltage (k_BT/q, ~26mV at room temperature), and n_i the intrinsic carrier concentration (~1.4×10^{10}cm^{-3}).

Fig. 7 shows the calculated square root of n_D as a function of V_B vs. the experimental measurements of η as of Fig. 6 (b) and of the variance of the V_{th0} distribution (σ^2_{Vth0}) as of Fig. 3 (note: the V_{th0}-variance is expected to follow the same technological dependences of η [16], cf. Eq. 2) . An excellent match is found over the whole considered range of V_B's, confirming that the improved time-zero and time-dependent variability obtained by applying a FBB are yielded by the reduced number of unscreened dopant atoms within the channel depletion region. Furthermore, 3D atomistic device simulations [17] confirm that the tail of the ΔV_{th} step height distribution is expected to be affected by BB. These findings suggest that, from the perspective of device variability, *the BB technique can be seen as a convenient and flexible electrical equivalent to doping adjustment.*

The time-dependent variability in nanoscaled devices leads to a shift in our perception of reliability: deterministic lifetimes measured on large area devices have to be replaced by lifetime distributions [3]: i.e., although the average reliability of a given

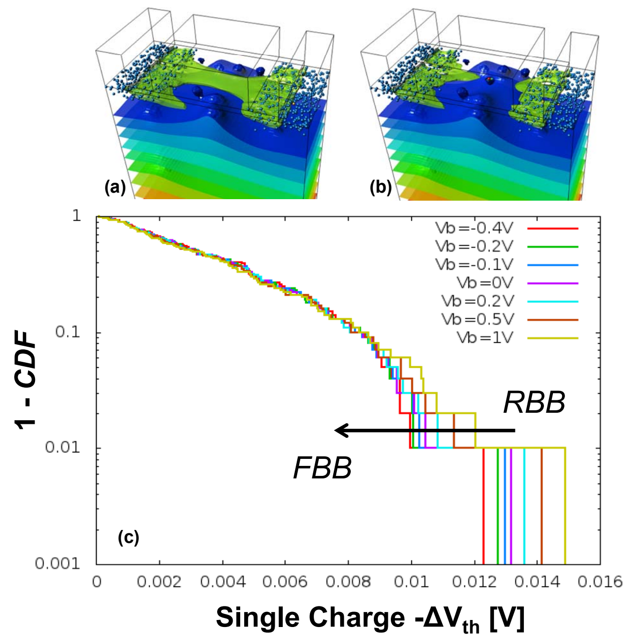

Figure 8. (a) 3D atomistic device simulation [17] showing a current percolation path in the channel due to potential non-uniformity caused by RDD; (b) The percolation path can be effectively switched off by a charged oxide defect located close to its confinement point. (c) ΔV_{th} step height distributions obtained by multiple 3D atomistic device simulations. The body bias is confirmed to modulate the distribution, with a FBB yielding a reduction of its tail and therefore a reduced time-dependent variability.

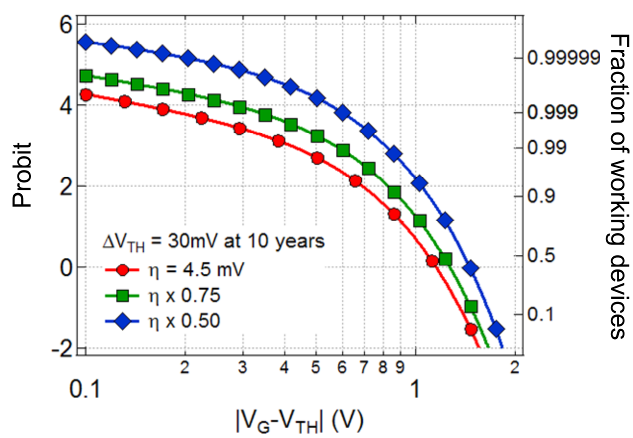

Figure 9. Fraction of working devices after 10 year of continuous operation at varying gate overdrive voltages (considered failure criterion: ΔV_{th}=30mV), calculated according to [18] for different η values. The reduction in η offered by the FBB technique projects to a significant improvement of the lifetime distribution of realistic device population.

technology might be sufficient, a fraction of a realistic device population (typically consisting of billions of devices) can still fail. It has been found that the average step height η is the key parameter controlling the lifetime distribution, while the average oxide defect density is of lesser relevance [18]. In this respect, the reduction in η offered by *the FBB technique projects to a significant improvement of the lifetime distribution* of realistic device populations (i.e. billions), as shown in Fig. 9.

Finally we note that the body bias experiments highlight the existence of a correlation between the time-zero variability (spread in V_{th0}) and the BTI-induced time-dependent variability (spread in ΔV_{th}). As previously shown by our group in [19], the distribution of the total ΔV_{th} induced by NBTI in nanoscaled devices can be analytically described by a convolution of the Poisson distribution describing the number of charging traps present in each device with the exponential distribution describing the impact per each charged trap (see Fig. 1b). As shown there, the variance of the total ΔV_{th} distribution is controlled by the parameter η (cf. Eq. 1-2) and increases with the stress time (i.e. the device use), or equivalently with the average induced $\langle \Delta V_{th} \rangle$ as:

$$\sigma^2_{\Delta Vth} = 2\eta \langle \Delta Vth \rangle \ . \quad (6)$$

Fig. 10 shows the standard deviation of the V_{th0} distribution measured for varying body biases as from Fig. 3, vs. the standard deviation of the BTI induced ΔV_{th} calculated by using Eq. 6 with the experimentally extracted η values as of Fig. 6, for an average induced $\langle \Delta V_{th} \rangle$ = 50mV (i.e. a typically considered device failure criterion). A correlation between the time-zero and time-dependent variability is apparent. Although the V_{th0} spread is larger than the ΔV_{th} spread (for the considered $\langle \Delta V_{th} \rangle$ = 50mV, $\sigma_{\Delta Vth} / \sigma_{Vth0}$=0.7), the relative importance of the time-dependent variability is expected to increase during the device lifetime (cf. Eq. 6). Moreover, the additional circuit design margin necessary to cope with the additional variability induced by BTI might become unsustainable when combined with the margin accounting for the significant time-zero variability in nanoscaled devices. In this scenario, the combined beneficial effects of a Forward Body Bias will become crucial.

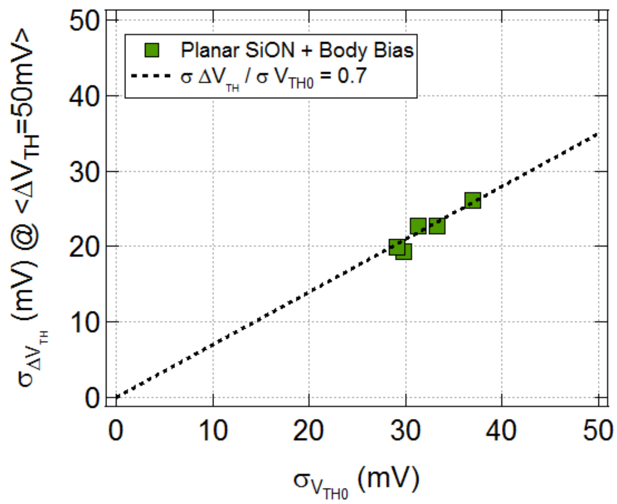

Figure 10. Spread of the initial threshold voltage distribution (σ_{Vth0}) plotted versus the spread of the total ΔV_{th} distribution ($\sigma_{\Delta Vth}$) after NBTI for different body biases.

V. Conclusions

The impact of individual charged gate oxide defects on nanoscaled pMOSFETs was studied as a function of the body bias. Modulations of both the time-zero variability and the time-dependent variability were found. These observations were explained by the modulation of the number of unscreened dopant atoms within the channel depletion region induced by the body bias. A forward body bias significantly reduces the average impact of individual gate oxide defects, and therefore constitutes a flexible electrical technique to improve the time-zero and the time-dependent variability in nanoscaled MOSFET devices without involving any technological tuning.

Acknowledgment

This work was performed as part of imec's Core Partner Program. It has been in part supported by the European Commission under the 7th Framework Programme (Collaborative project MORDRED, contract No. 261868). Discussions with Dr. H. Reisinger are gratefully acknowledged.

References

[1] A. Asenov, R. Balasubramaniam, A. R. Brown, and J. H. Davies, "RTS Amplitude in Decananometer MOSFETs: 3-D Simulation Study", in *IEEE* Trans. Electron Devices, Vol. 50, no. 3, 2003, pp. 839-845;

[2] V. Huard *et al.*, "NBTI Degradation: from Transistor to SRAM Arrays", in *Proc. IEEE* International Reliability Physics Symposium, 2008, pp. 289-300;

[3] B. Kaczer *et al.*, "Origin of NBTI Variability in Deeply Scaled pFETs", in *Proc. IEEE* International Reliability Physics Symposium, 2010, pp. 26-32;

[4] M. Toledano-Luque *et al.*, "Response of a Single Trap to AC Negative Bias Temperature Stress, in *Proc. IEEE* International Reliability Physics Symposium, 2011, pp. 364-371;

[5] V. Huard, F. Cacho, Y. Mamy Randriamihaja, A. Bravaix, "From Defects Creation to Circuit Reliability", in Microelectronic Engineering, Vol. 88, no. 7, 2011, pp. 1396-1407;

[6] T. Grasser *et al.*, "Recent Advances in Understanding the Bias Temperature Instability", in *Proc. IEEE* International Electron Device Meeting, 2010, pp. 82-85;

[7] C. Liu *et al.*, "New Observations on AC NBTI induced Dynamic Variability in Scaled High-κ / Metal-gate MOSFETs: Characterization, Origin of Frequency Dependence, and Impacts on Circuits", in *Proc. IEEE* International Electron Device Meeting, 2012, pp. 466-469;

[8] J. Franco *et al.*, "Impact of Single Charged Gate Oxide Defects on the Performance and Scaling of Nanoscaled FETs", in *Proc. IEEE* International Reliability Physics Symposium, 2012, pp. 5A.4.1-6;

[9] B. Kaczer *et al.*, "The Relevance of Deeply-Scaled FETs Threshold Voltage Shift for Operation Lifetime", in *Proc. IEEE* International Reliability Physics Symposium, 2012, pp. 5A.2.1-6 ;

[10] A. Ghetti, C.M. Compagnoni, A.S. Spinelli, A. Visconti, "Comprehensive Analysis of Random Telegraph Noise Instability and Its Scaling in Deca-Nanometer Flash Memories", in *IEEE* Trans. Electron Devices, Vol. 56, no. 8, 2009, pp. 1746-1752;

[11] http://www.ibiblio.org/e-notes/Perc/contour.htm;

[12] A. Hokazono *et al.*, "Forward Body Biasing as a Bulk-Si CMOS Technology Scaling Strategy", in *IEEE* Trans. Electron Devices, Vol. 55, no. 10, 2008, pp. 2657-2664;

[13] N.B. Lukyanchikova, M.V. Petrichuk, N.P. Garbar, E. Simoen, C. Claeys, "Influence of the substrate voltage on the random telegraph signal parameters in submicron *n*-channel metal-oxide-semiconductor field-effect transistors under a constant inversion charge density", Appl. Phys. A, Vol. 70, 2000, pp. 345-353;

[14] Y. Mitani, H. Satake, and A. Toriumi, "Influence of Nitrogen on Negative Bias Temperature Instability in Ultrathin SiON", in *IEEE* Trans. Device and Material Reliability, Vol. 8, No. 1, pp. 6-13, 2008;

[15] N. Arora, "MOSFET Modeling for VLSI Simulation—Theory and Practice", World Scientific Publishing Co. Pte. Ltd., ISBN 978-981-256-862-5, 1992;

[16] K.J. Kuhn *et al.*, "Process Technology Variation", in *IEEE* Trans. Electron Devices, Vol. 58, no. 8, 2011, pp. 2197-2208;

[17] B. Schwarz *et al.*, "Electrostatic Properties of Single and Multiple Charged Oxide Traps in the Presence of Random Discrete Dopants", submitted;

[18] M. Toledano-Luque *et al.*, "From Mean Values to Distributions of BTI Lifetime of Deeply Scaled FETs through Atomistic Understanding of the Degradation", in *Proc.* VLSI Symp. 2011, pp. 152-153;

[19] B. Kaczer, Ph.J. Roussel, T. Grasser, and G. Groeseneken, "Statistics of Multiple Trapped Charges in the Gate Oxide of Deeply Scaled MOSFET Devices—Application to NBTI", in *IEEE* Electron Device Letters, Vol. 31, no. 5, 2010, pp. 411-413.